Received: 11 May 2021 | Revised: 15 September 2021 | Accepted: 28 September 2021

DOI: 10.1002/er.7368

RESEARCH ARTICLE

INTERNATIONAL JOURNAL OF ENERGY RESEARCH WILEY

Thermophysical properties and thermal performance evaluation of multiwalled carbon nanotube-based organic phase change materials using T-History method

Chandrmani Yadav | **Rashmi Rekha Sahoo**

Department of Mechanical Engineering, Indian Institute of Technology (BHU), Varanasi, India

Correspondence
Rashmi Rekha Sahoo, Department of Mechanical Engineering, Indian Institute of Technology (BHU), Varanasi 221005, India.
Email: rrs_iitbhu@rediffmail.com

Summary

Experimental studies have been carried out to evaluate the thermophysical properties and thermal performance of thermal energy storage (TES) systems. The TES system was filled with 0%-0.025% vol. fractions multiwalled carbon nanotubes (MWCNT)-based lauric acid (LA), paraffin wax (PW), and stearic acid (SA) nanoparticle-enhanced phase change materials (NEPCMs). The T-History method has been used to explore the thermophysical parameters, i.e., solid-liquid specific heat capacity, solid-liquid thermal conductivity, and heat of fusion. Results revealed that the solid thermal conductivity of the 0.02% MWCNT in lauric acid, paraffin wax, and stearic acid increased by 37.8%, 24.4%, and 13.5% than LA, PW, and SA phase change materials (PCMs), respectively. Also, an improvement in liquefying and solidification time has been observed for 0.02% vol. fraction MWCNT-based NEPCMs. However, the dimensionless numbers justified that the combined conduction and natural convection effect occurred in the PCMs/NEPCMs thermal energy storage. The coefficient and rate of heat transfer have been compared among 0%-0.025% vol. fraction of MWCNT-based pure lauric acid, paraffin wax, and stearic acid PCMs/NEPCMs. Also, the maximum heat transfer rate for 0.02% MWCNT in lauric acid, paraffin wax, and stearic acid NEPCMs has been increased by 61.16%, 87%, and 26.4%, respectively, compared to LA, PW, and SA phase change materials. Hence, the 0.02% MWCNT/PW-NEPCM-based TES system has higher performance than the mentioned TES systems.

KEYWORDS

heat transfer rate, lauric acid, melting-solidification time, multiwall carbon nanotubes, paraffin wax, stearic acid

1 | INTRODUCTION

Uncontrolled fossil usage has led to severe problems like global warming, the release of carbon dioxide (CO_2), nitric oxide (NOx), sulfur dioxide (SOx), and other harmful gases in the environment. There is an urgent need to address the problem of the energy crisis. Renewable energy is an excellent source to meet energy scarcity. But most renewable energy sources are unreliable due to their dependence on the season and weather. Thus, waste heat recovery is an economical method to cater to the

Abbreviation: NEPCM, nanoparticle-enhanced phase change materials.

demand for energy. Waste heat accessories can be applied to internal combustion engines, power plants, cement-producing industries, etc.[1,2] Different waste heat recovery methods are available in the literature for specific applications. For instance, an organic Rankine cycle can extract the industrial waste heat and heat from heavy-duty engines. Despite a variety of methods available, each method has its advantages and disadvantages. The use of a thermal energy storage system (TES) is one such method. Mainly, organic-inorganic and bio-based-type phase change materials are applied in thermal energy storage (TES). The global thermal energy storage market reported that from an anticipated United States dollar (USD) 188 million in 2020, it is expected to grow at 14.4% to (USD)369 million by 2025. Increased need for electricity during peak hours, increasing commercialization of concentrating solar power (CSP) plants, and demand for heating and cooling applications for smart infrastructure are all propelling the worldwide thermal energy storage market ahead.[3] Also, from 2010 to 2015, the global phase change material market is predicted to increase at a CAGR of 31.7%, from (USD)300.8 million in 2009 to (USD) 1488.1 million in 2015. The global phase change material market was expected to grow from $300.8 million in 2009 to $1488.1 million in 2015, at an estimated compound annual growth rate (CAGR) of 31.7% from 2010 to 2015.[4] In the TES system, a portion of exhaust waste energy was recovered[5-8] by storing it in phase change materials (PCM). The advantages of using such a system are compact, reliable, and economical. Despite several advantages, the efficiency of such systems is low. Thus, to compete with existing waste heat recovery methods, the efficiency of such a system should be improved.

Various pathways are available in the literature to enhance the efficiency of the TES-based system. The most critical parameter of the TES system is the thermophysical properties of the PCM. Different strategies have been proposed to improve thermophysical properties. The use of hybrid-type PCMs in place of normal PCMs is one such method. Karthik et al[9] worked on erythritol-graphite foam as a hybrid composite PCM. Using erythritol-graphite foam in the TES system, the thermal conductivity has been enhanced five times than erythritol. Kumar et al[10] investigated eutectic compositions such as lauric acid, myristic acid (MA), and palmitic acid (PA) with 1-dodecanol. They concluded that the melting temperatures and latent heat for LA, MA, and PA with eutectic compositions are 17°C, 18.43°C, 20.08°C, and 175, 180, 190 kJ/kg, respectively. However, in this case, at a low melting temperature between 17°C and 20°C, comparatively shows higher latent heat. Paola et al[11] prepared Glauber's salt-based PCMs by using bentonite and borax. Also, the thermal performance and stability of PCMs were crossed and analyzed by the T-history method and an optical light scattering method. Results revealed that by increasing the bentonite in Glauber's salt-based PCM, less heat was released to the environment, but higher heat was required for solidification. However, a less homogenous sample was obtained with a lower amount of water in PCM, which was observed by the backscattering profile. It may happen due to an ineffective sonication process, which results in less thermal efficiency. Paola et al[12] worked on the thermal performance analysis of the three different cooling chambers considering eight samples of salt-based PCMs. Results revealed that the cooling rate did not affect the initial temperature and specific heat but strongly influenced the solidification enthalpy. Also, the solidification enthalpy increased by an increment in water, bentonite, and borax in the composition of Glauber's salt-based PCMs. Paola and Lopresto[13] investigated an alternative of organic-inorganic PCMs by waste oils and its products as bio-based PCMs. The low thermal physical properties of conventional PCMs were reduced by bio-based PCMs and gave better air conditioning systems and refrigeration applications. Li et al[14] constructed a nanofibril/silver nanowire hybrid that added anisotropy-functionalized cellulose-based PCMs. These composite PCMs result in an improved value for thermal conductivity, thermal enthalpy, shape, and thermal stability, which enhanced the conversion and storage capacity of the solar-thermal energy system.

Another necessary means to enhance the efficiency of the TES system is based on improvement in the design of the TES system. Yazici et al[15] analyzed the performance of the PCM/graphite matrix in a horizontal tube in a shell-type TES system. The performance has been enhanced by decreasing melting time. The effective thermal conductivity was increased by 35 times that of pure paraffin wax. Researchers have also improved the thermal performance of the TES system by applying fins. Francis et al[16] used longitudinal fins type TES system and reduced charging time and subcooling problem during discharging period. Jaume et al[17] enhanced 4.7-9.4 times performance by using a fin-type TES system than the heat transfer surface. Veismoradi et al[18] done numerical simulation using the FEM on a shell-tube TES system filled with copper metal foam. The vertical arrangement of tubes in the TES system showed that melting would be advanced by 80%. Zhou et al[19] designed new parameter areas above and below the inner tube, "eccentric space ratio," as an approximation of the ratio of the area to measure the degree of eccentricity. The melting and solidification times will be advanced by 40% and 45%, respectively, between 4:1 and 14:1 different radius ratios.

Demirkıran and Cetkin[20] compared eccentric two tubes with rectangular shells and concentric tubes with circular shells. It was observed that melting time and sensible energy in eccentric two tubes with the rectangular shell are decreased in comparison to the concentric tubes with the circular shell. Asgari et al[21] investigated the effect of fins with different thicknesses and lengths on the thermal conductivity of PCMs. They concluded that the lower thickness of the fin is a more viable option for increasing the heat transfer rate.

Researchers have also proposed the use of nano-additives in PCMs for the enhancement of thermophysical properties. Yadav and Sahoo[22] investigated that an addition of 0.1% volume fraction aluminum oxide (Al_2O_3) nano-additives in lauric acid, the charging time, energy, and exergy saved was enhanced by 16.13%, 38.71%, 5.84%, 6.27%, 34.24%, and 35.22% compared to pure lauric acid and paraffin wax PCM, respectively. Also, Yadav and Sahoo[23] worked on stearic acid PCM with 0%-0.5% mass fractions of Al_2O_3. The energy transfer rate of 0.3% mass fraction Al_2O_3 nano-additives-based stearic acid NEPCM was observed to be higher than 11.08% than the stearic acid-based TES system. Sopian et al[24] carried out the experimental and parametric analysis on a photovoltaic thermal collectors system with nano-PCM and nanofluid as the heat transfer fluid. Results revealed that the average and peak overall photovoltaic thermal efficiencies had been improved, and also the electrical efficiency of the photovoltaic thermal was higher than photovoltaic. Lin et al[25] used microencapsulated phase change materials as an energy storage material. It solved the problems of leakage during phase change, poor cycle stability, low encapsulation efficiency, and a high degree of supercooling. Yu et al[26] worked on composite shape-stable PCM, that is, $MgCl_2$ -NaCl-KCl, expanded graphite, and silicon dioxide (SiO_2) nanoparticles. However, the expanded graphite used for shape stability and SiO_2 nanoparticles improved the thermophysical properties of PCM—the composite PCM showed an increment in specific heat capacity and thermal conductivity. Also, the use of single-walled carbon nanotubes (SWCNT)and MWCNT in PCMs revealed impressive results. Yu et al[27] investigated that the addition of single-walled carbon nanotubes in sodium chloride (NaCl)-based molten salt reduced the melting point temperature and heat of fusion by 36.37%. Also, by increasing the amount of SWCNT, the thermophysical properties both enhanced. However, after a certain volume fraction of based composite PCMs, the thermophysical properties were reduced due to the dispersion problem of SWCNT/MWCNT in based PCM. Yadav and Sahoo[28] investigated that after an optimum value of volume fraction of carbon nanotubes in PCM, the thermophysical properties were decreased. The thermal conductivity of 0.02% MWCNT-capric acid (CA) PCM was 31.29% higher than CA, respectively. Yadav and Sahoo[29] investigated the performance of the TES system filled with 0.02% carbon tubes based on capric acid PCM and concluded that 61.9% and 70.92% of the energy and exergy storage medium had been observed for 0.02% MWCNT in capric acid, respectively. Deqiu Zou et al[30] worked on MWCNT/graphene-based PCM and revealed that the 3/7 ratio of MWCNT/graphene-based PCM has 31.8%, 55.4%, and 124% higher thermal conductivity than graphene-based PCM, MWCNT-based PCM, and pure PCM, respectively. Li et al[14] investigated that with porous cellulose nanofibrils (CNF)/silver nanowire (AgNW) composite PCMs, an increment of 72.7% in thermal conductivity is observed. Li et al[31] compared with and without carbon nanotubes high-density polyethylene/paraffin wax and concluded that the thermal and electrical conductivity of carbon nanotubes-based polyethylene/paraffin wax is improved. However, the above kinds of literature summarize that the addition of MWCNT in PCM enhances the overall thermal properties, i.e., thermal conductivity and heat storage enthalpy. Also, MWCNT nanoadditives showed uniform dispersion throughout the composition and had better cycling performance with thermal stability.

In an earlier study, capric acid PCM was used for waste heat recovery due to its thermophysical properties, which were suitable for low-temperature heat recovery only (up to 32°C). In this study, the scope of the system has been increased for the heat up to 80°C, which is

TABLE 1 Properties of lauric acid, paraffin wax, stearic acid PCM, and MWCNT nanoparticles

Properties	LA[32]	PW[22]	SA[33]	MWCNT nanoparticles[28]
h_{ls} (kJ/kg)	152-162	243.5	186.5-210	-
K (W/m K)	0.15-0.16	0.15	0.097-0.172	2000
C_p (kJ/kg K)	1.8-2.1 (s), 2.1 (l)	2.89 (s)	2.07-2.83 (s) 1.9-2.38 (l)	0.733
ρ (kg/m^3)	1001 (s), 852-885	809.5 (s)-771 (l)	941-965 (s) 839-848 (l)	2100
μ (mPa s)	7.30	6.89	7.79	-

suitable for the heat recovery from automobiles. The three chosen PCMs (lauric acid, paraffin wax, and stearic acid) have been investigated due to their higher melting temperature. The thermophysical property of the MWCNT-based three PCMs has been improved for enhanced heat recovery of the TES system. The volume fraction of MWCNT has varied from 0% to 0.025%, and the effect on thermophysical properties has been assessed using the T-History method and hot disk analyzer. However, the drastic improvement in thermal performance has been observed by the variation in volume fraction from 0% to 0.02% of MWCNT-based NEPCMs. With the addition of MWCNT from 0.02% to 0.025% vol. fraction in PCMs, the thermophysical properties of NEPCMs have been decreased. Also, the performance of the TES system has been reduced due to the settlement of MWCNT particles. Among all samples, 0.02% volume fraction of MWCNT-based paraffin wax NEPCMs has shown an optimum enhancement in the thermophysical properties for NEPCMs.

2 | DESCRIPTION OF THE EXPERIMENT

2.1 | Materials

LA (pure) and SA (pure) have been purchased from Sisco research laboratories private limited. PW (with ≤0.05% sulfated ash) and multiwalled carbon nanotube (purity-99%) were purchased from Merck life science Private Limited and Shilpa enterprises. Table 1 shows the thermo-physical properties of LA, PW, SA, and MWCNT.

2.2 | Methods

2.2.1 | Preparation of MWCNT-based NEPCMs

The preparation of MWCNT within the volume fraction range of 0% to 0.025%-based LA, PW, and SA PCMs/NEPCMs were based on a two-step method. In this method, the MWCNT was mixed with PCMs at melting temperature. The mixtures have been stirred with a magnetic stirrer for 1 hour at the melting temperature of PCMs. After then, at room temperature, the samples of NEPCMs have solidified. It is observed that volume fraction above 0.02% of MWCNT, some particles of MWCNT settled at the bottom of the test tube. Also, the particles aggregation problems can be prevented by increasing the sonication period, the addition of stabilizers such as span 80, or other advanced methods like force steric stabilization, which involves an alteration of surface chemistry.

2.2.2 | T-History method

The T-History method is a very conventional, simple, inexpensive, fast, and helpful method for measuring thermo-physical properties of any pure or additives-based

TABLE 2 Specification of the TES system

Parameters	Diameter (m)	Length (m)	Specific heat capacity(kJ/kg K)	Thermal conductivity (W/m K)	Density (kg/dm)
Borosilicate breaker	0.145	0.185	0.8	1.2	223
Glass test tube	0.02	0.18	0.8	1.2	223

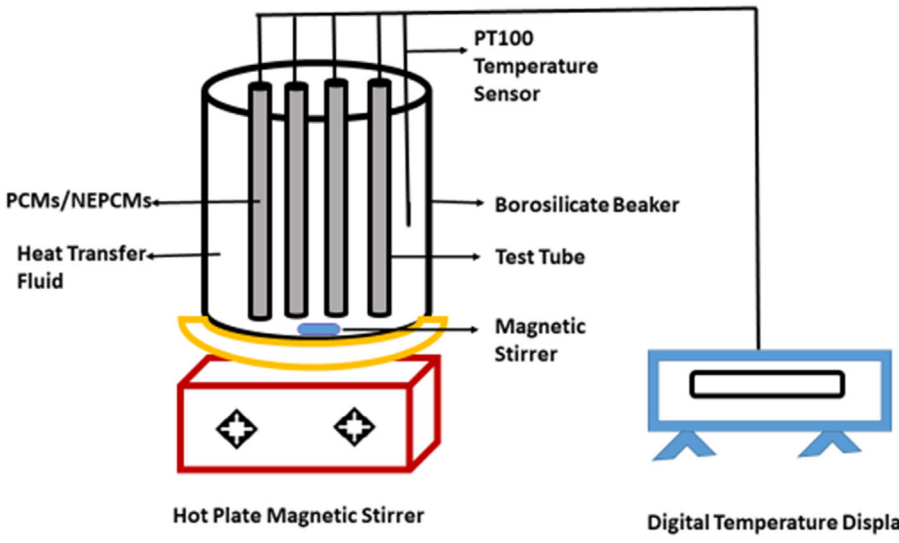

FIGURE 1 The schematic diagram of an experimental setup

TABLE 3 Accuracy of instruments

Instrument	Value
Stopwatch	±0.2%
Digital weighing machine	±0.4%
Measuring flask	±0.3%
Thermocouple	±0.5°C

TABLE 4 Calculated maximum uncertainties

Parameters	Uncertainties
Temperature	±1%
Mass m	±0.8%
Area A	±0.14%
Specific heat capacity	±2.1%
Thermal conductivity	±2.7%
Heat of fusion	±3.4%
Heat transfer coefficient	±1.2%
Heat transfer rate	±1.6%

materials. The standard tools such as differential scanning calorimetry (DSC) and differential thermal analysis (DTA) are limited to small material samples, which need a high precision sampling of the material. Zhang and Jiang[34] proposed the T-History method. Thermo-physical properties such as latent heat of fusion, specific heat (liquid/solid), and thermal conductivity (liquid/solid) of actual bulk PCM with or without additives were calculated by the T-History method without sampling steps. The reference material must be fulfilled the lumped capacity method (Bi <0.1). In this method, two vertical test tubes are required and the first test tube was filled with PCM melted at a constant temperature bath, which was higher than the melting temperature of PCM. The second test tube was filled with distilled water as reference material. Afterward, both test tubes were removed from the bath and cooled in the surrounding. The temperature profile of materials and surrounding test tubes were recorded by the temperature measuring devices.

Based on these temperature profiles, three areas were observed between the PCM and ambient air temperature profile. These areas are indicated as the liquid zone,

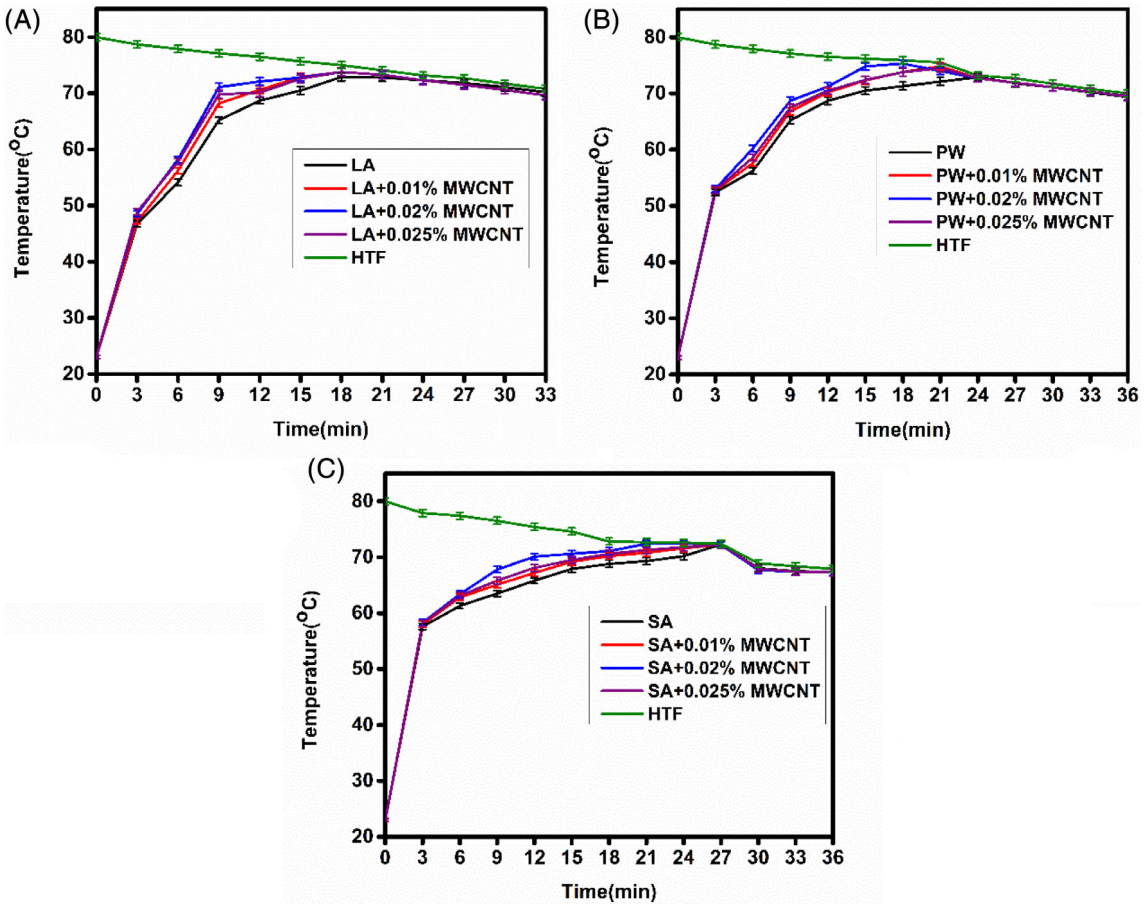

FIGURE 2 A, Charging profile of lauric acid PCM/NEPCM. B, Charging profile of paraffin wax PCM/NEPCM. C, Charging profile of stearic acid PCM/NEPCM

liquid-solid zone, and solid zone. Similarly, these areas also represent the reference material with respect to PCM. However, by putting the values in given empirical equations (from Equations (4) to (9)), the thermo-physical properties were calculated by simple calculation of mathematics.

2.2.3 | Test description

The pure and MWCNT-based PCMs/NEPCMs were filled in glass test tubes at ambient temperature. The loaded test tubes with the volume fraction from 0, 0.01%, 0.02%, and 0.025% MWCNT-based LA, PW, and SA composite PCMs have been heated with the help of hot water as a heat transfer fluid (HTF) in a borosilicate beaker. The HTF was heated from 20°C to 80°C by a hot plate magnetic stirrer. Table 2 shows the specification of the experimental instruments. With the help of a PT100 coupled to a digital temperature display meter, the temperature of the TES system was measured. Every 3 and 5 minutes time slot, the charging and solidification temperatures of PCMs/NEPCMs have been recorded. The temperature range of PT100 is from −200°C to 850°C. Figure 1 shows a schematic diagram of the experimental setup.

2.3 | Uncertainties analysis

The uncertainties analysis for the prediction in parameters was calculated by using Holman et al[35] Equations (1) and (2). Where P is the measured value, which was dependent on unrelated measured parameters Q_1, Q_2, Q_3 ...Q_n and R_1, R_2, R_3...R_n is the uncertainties in the independent variables.

$$P = P\left(Q_1^{R_1}, Q_2^{R_2}, Q_3^{R_3} \ldots\ldots\ldots Q_n^{R_n}\right) \tag{1}$$

Then the uncertainties (U_S) can be expressed by[36]:

$$U_S = \sqrt{\left[\left(\frac{\partial P}{\partial Q_1}R_1\right)^2 + \left(\frac{\partial P}{\partial Q_2}R_2\right)^2 + \left(\frac{\partial P}{\partial Q_3}R_3\right)^2 + \ldots\ldots\ldots\ldots\left(\frac{\partial P}{\partial Q_n}R_n\right)^2\right]} \tag{2}$$

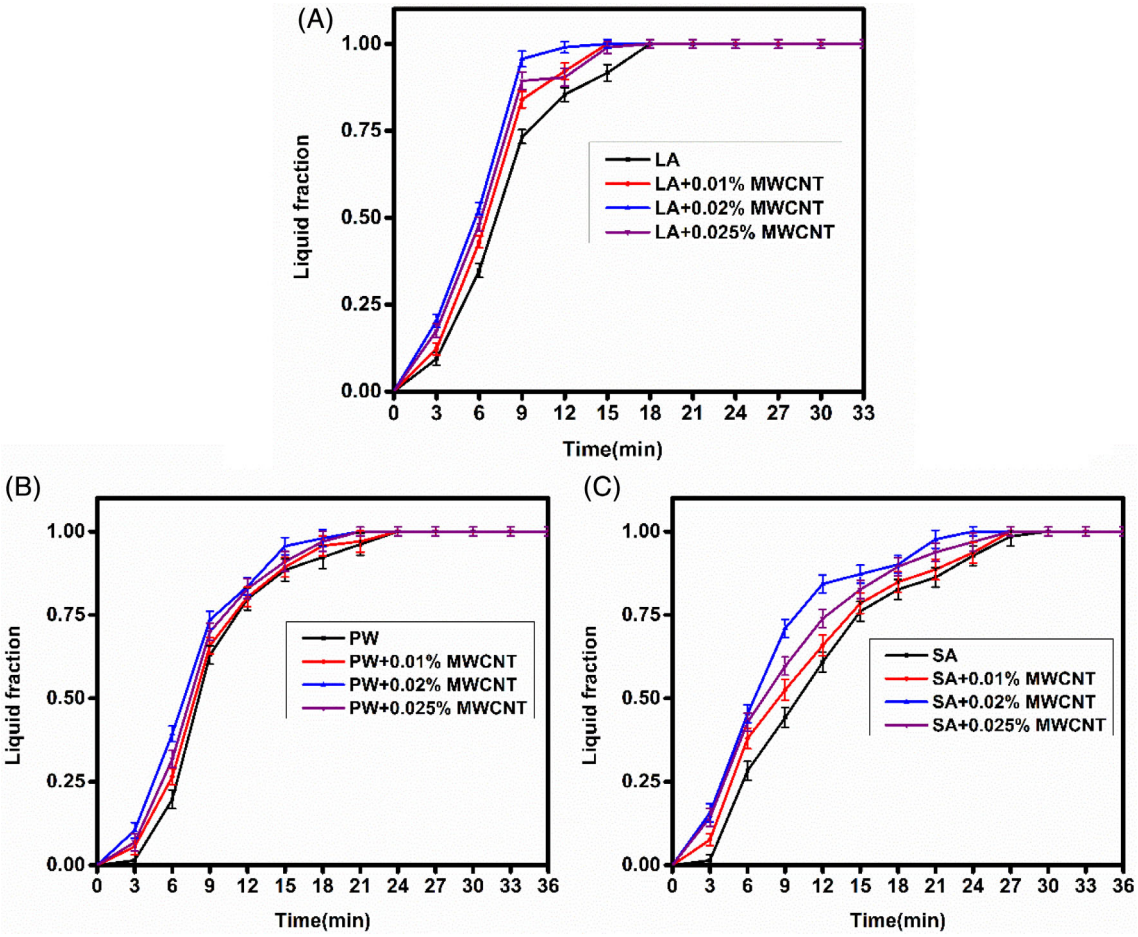

FIGURE 3 A, The liquid fraction of lauric acid PCM/NEPCM. B, The liquid fraction of paraffin wax PCM/NEPCM. C, The liquid fraction of stearic acid PCM/NEPCM

Tables 3 and 4 are showing the accuracy of instruments and maximum uncertainties of parameters, respectively.

2.4 | Data reduction

By using the charging temperature profile of PCMs/NEPCMs, the liquid fraction has been observed. Dimensionless numbers such as Fourier numbers and Rayleigh numbers justified the mode of the heat transfer process. The thermophysical properties of MWCNT-based NEPCMs have been established by the T-History method.[34] In the T-History method, a solidification temperature profile of PCMs/NEPCMs would be required. Furthermore, based on the thermophysical properties, the thermal performance of the TES system filled with PCMs/NEPCMs has been investigated.

The liquid fraction (f) of PCMs/NEPCMs filled in TES system can be expressed as[37]:

$$f = \begin{cases} 0, \text{if } T < T_s \\ \dfrac{T - T_s}{T_l - T_s}, \text{if } T_s < T < T_l \\ 1, \text{if } T > T_l \end{cases} \quad (3)$$

The specific heat capacity of solid-phase PCMs/NEPCMs can be expressed by the T History method as[34]:

$$c_{ps} = \frac{m_w c_{pw} + m_t c_{pt}}{m_p} \times \frac{A_3}{B_2} - \frac{m_t}{m_p} \times c_{pt} \quad (4)$$

The specific heat capacity of liquid phase PCMs/NEPCMs expressed by the T History method as[34]:

$$c_{pl} = \frac{m_w c_{pw} + m_t c_{pt}}{m_p} \times \frac{A_1}{B_1} - \frac{m_t}{m_p} \times c_{pt} \quad (5)$$

The thermal conductivity of solid-phase PCMs/NEPCMs expressed by the T History method as[34]:

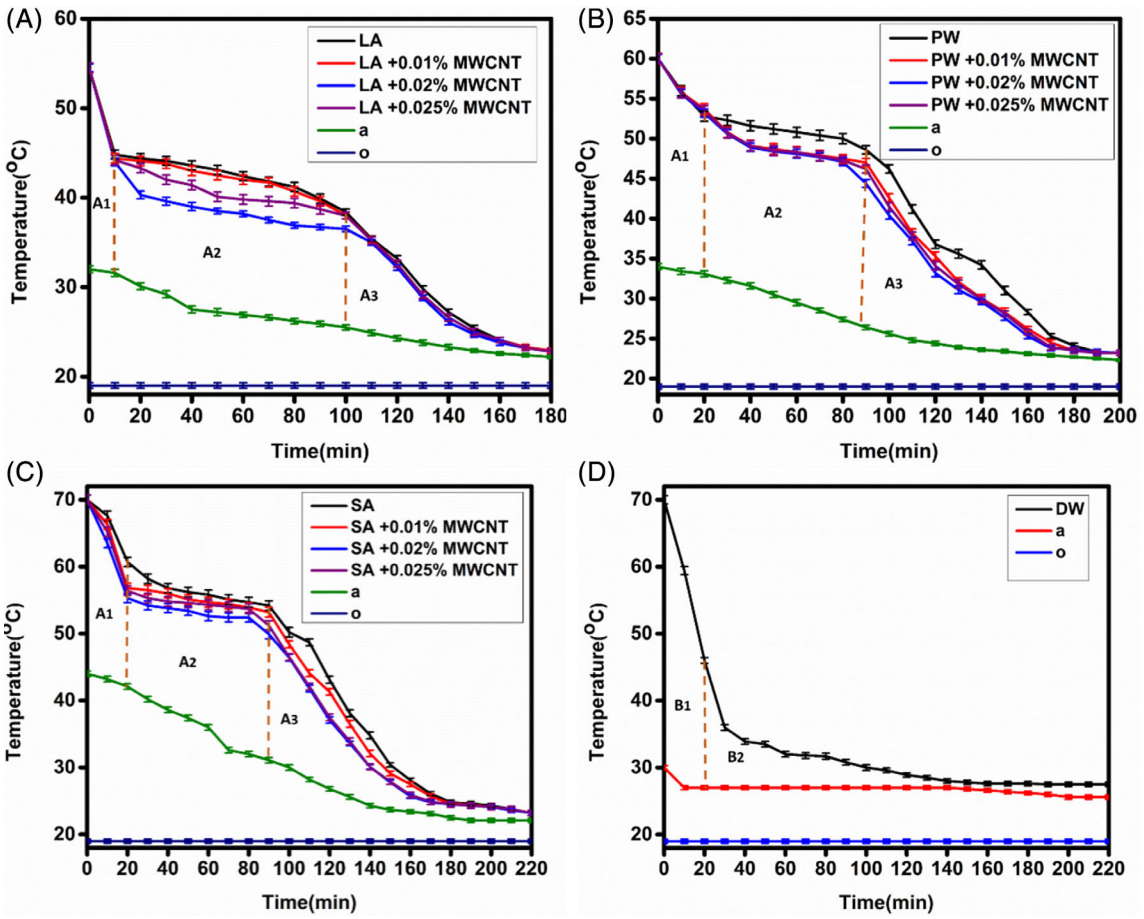

FIGURE 4 A, The solidification profile of lauric acid PCM/NEPCM. B, The solidification profile of paraffin wax acid PCM/NEPCM. C, The solidification profile of stearic acid PCM/NEPCM. D, The temperature of distilled water during the cooling process

$$k_s = \left[1 + \frac{c_{ps}}{h_{ls}} \times (T_m - T_w)\right] / 4 \left[\frac{t_f}{\rho_p R^2 h_{ls}} \times (T_m - T_w) - \frac{1}{h_w R}\right] \quad (6)$$

The thermal conductivity of liquid-phase PCMs/NEPCMs expressed by the T History method as[34]:

$$k_l = \left[1 + \frac{c_{pl}}{h_{ls}} \times (T_m - T_w)\right] / 4 \left[\frac{t_f}{\rho_p R^2 h_{ls}} \times (T_m - T_w) - \frac{1}{h_w R}\right] \quad (7)$$

The latent heat (h_{ls}) of pure form of PCMs shown by the T History method as[34]:

$$h_{ls} = \frac{m_w c_{pw} + m_t c_{pt}}{m_p} \times \frac{A_2}{B_1} \times (T_o - T_s) \quad (8)$$

The latent heat (h_{ls}) of NEPCMs shown by[34]:

$$h_{ls} = \frac{m_w c_{pw} + m_t c_{pt}}{m_p} \times \frac{A_2}{B_1} \times (T_o - T_s) - \frac{m_t c_{pt}}{m_p} \times (T_{f1} - T_{f2}) \quad (9)$$

where T_{f1} and T_{f2} are the temperature range during the phase-change process.

The Fourier number (Fo) of pure and MWCNT-based PCMs/NEPCMs can be expressed as:

$$Fo = \alpha t / l^2 \quad (10)$$

where thermal diffusivity, $\alpha = k/\rho c_p$.

Also, the Rayleigh number (Ra) of pure and MWCNT-based PCMs/NEPCMs can be expressed as[38]:

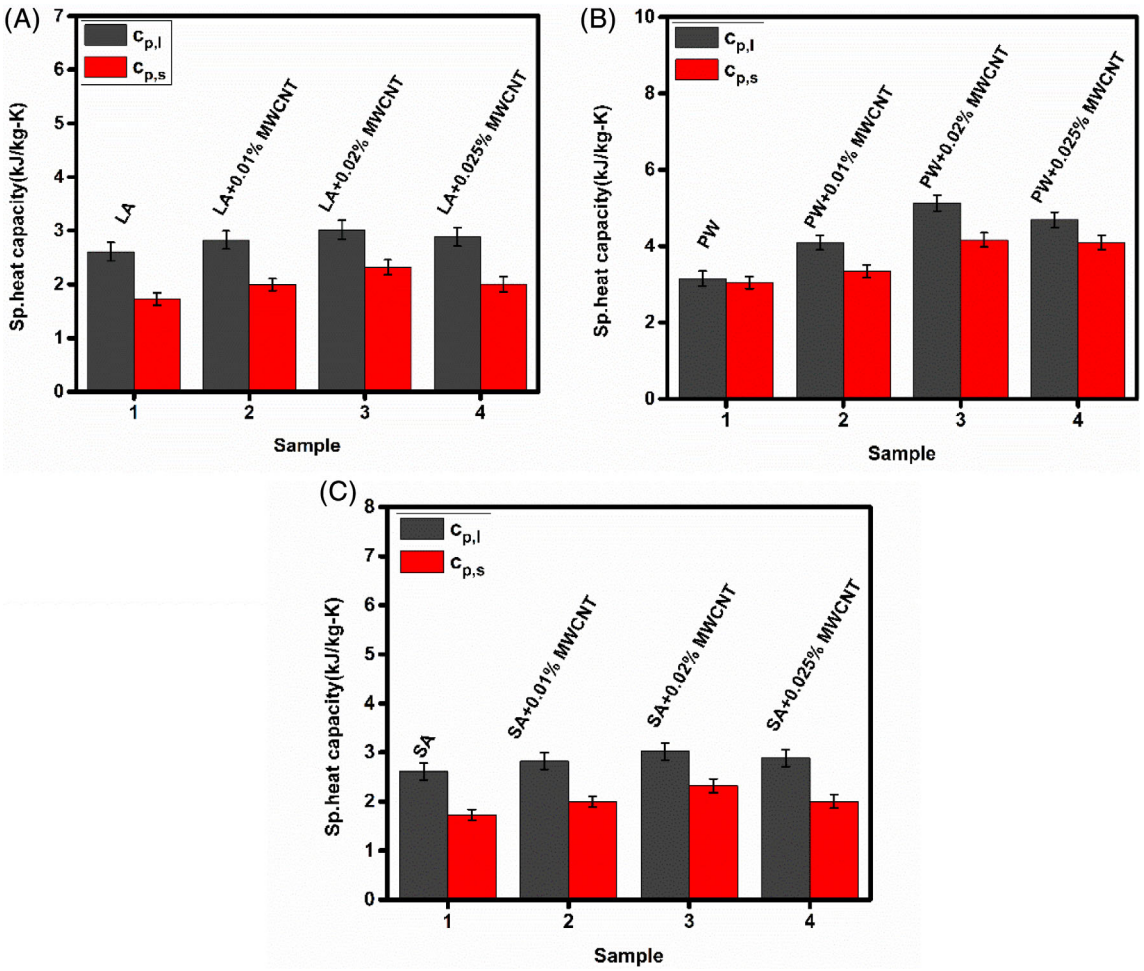

FIGURE 5 A, The specific heat capacity of lauric acid PCM/NEPCM. B, The specific heat capacity of paraffin wax PCM/NEPCM. C, The specific heat capacity of stearic acid PCM/NEPCM

$$\mathrm{Ra} = \frac{g\rho\beta l^3 (T_\mathrm{W} - T_\mathrm{m})}{\alpha\mu} \tag{11}$$

The Nusselt number (Nu) of pure and MWCNT-based PCMs/NEPCMs filled in the TES system can be expressed as[38]:

$$\mathrm{Nu} = 0.59 \times \mathrm{Ra}^{0.25} \tag{12}$$

The heat transfer coefficient (h) for TES system filled with PCMs/NEPCMs can be expressed as:

$$h = \frac{\mathrm{Nu} \times k}{l} \tag{13}$$

The heat transfer rate (Q) from water to PCMs/NEPCMs can be expressed as:

$$Q = \mathrm{hA}(T_\mathrm{w} - T_\mathrm{R}) \tag{14}$$

where cross-section area of the tube, $A = 2\pi R \times l$

The volume fraction (ϕ) of MWCNT in PCMs can be expressed as[39]:

$$\phi[\%] = \left[\frac{\frac{W_{np}}{\rho_{np}}}{\frac{W_{np}}{\rho_{np}} + \frac{W_p}{\rho_p}}\right] \times 100 \tag{15}$$

The density of MWCNT-based NEPCMs (ρ_{nep}) can be expressed as[40]:

$$\rho_{\mathrm{nep}} = (1-\phi)\,)\rho_\mathrm{p} + \phi\rho_{\mathrm{np}} \tag{16}$$

The dynamic viscosity of MWCNT-based NEPCMs (μ_{nep}) can be expressed as[40]:

$$\mu_{\mathrm{nep}} = \frac{\mu_\mathrm{p}}{(1-\phi)^{2.5}} \tag{17}$$

The expansion coefficient of MWCNT-based NEPCMs (β_{nep}) can be expressed as[40]:

$$\beta_{nep} = \frac{(1-\phi)(\rho\beta)_\mathrm{p} + \phi(\rho\beta)_{\mathrm{np}}}{\rho_{\mathrm{np}}} \tag{18}$$

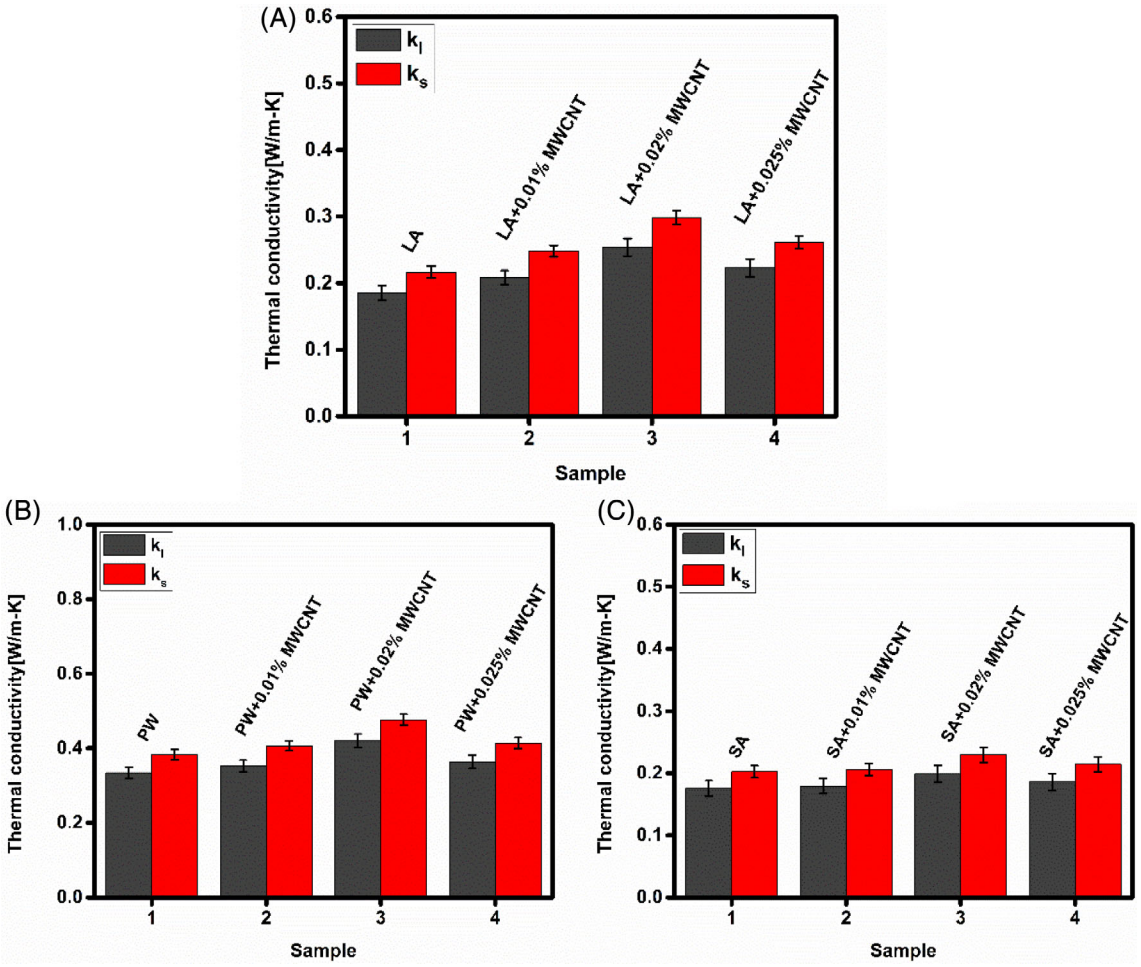

FIGURE 6 A, The thermal conductivity lauric acid PCM/NEPCM. B, The thermal conductivity paraffin wax PCM/NEPCM. C, The thermal conductivity stearic acid PCM/NEPCM

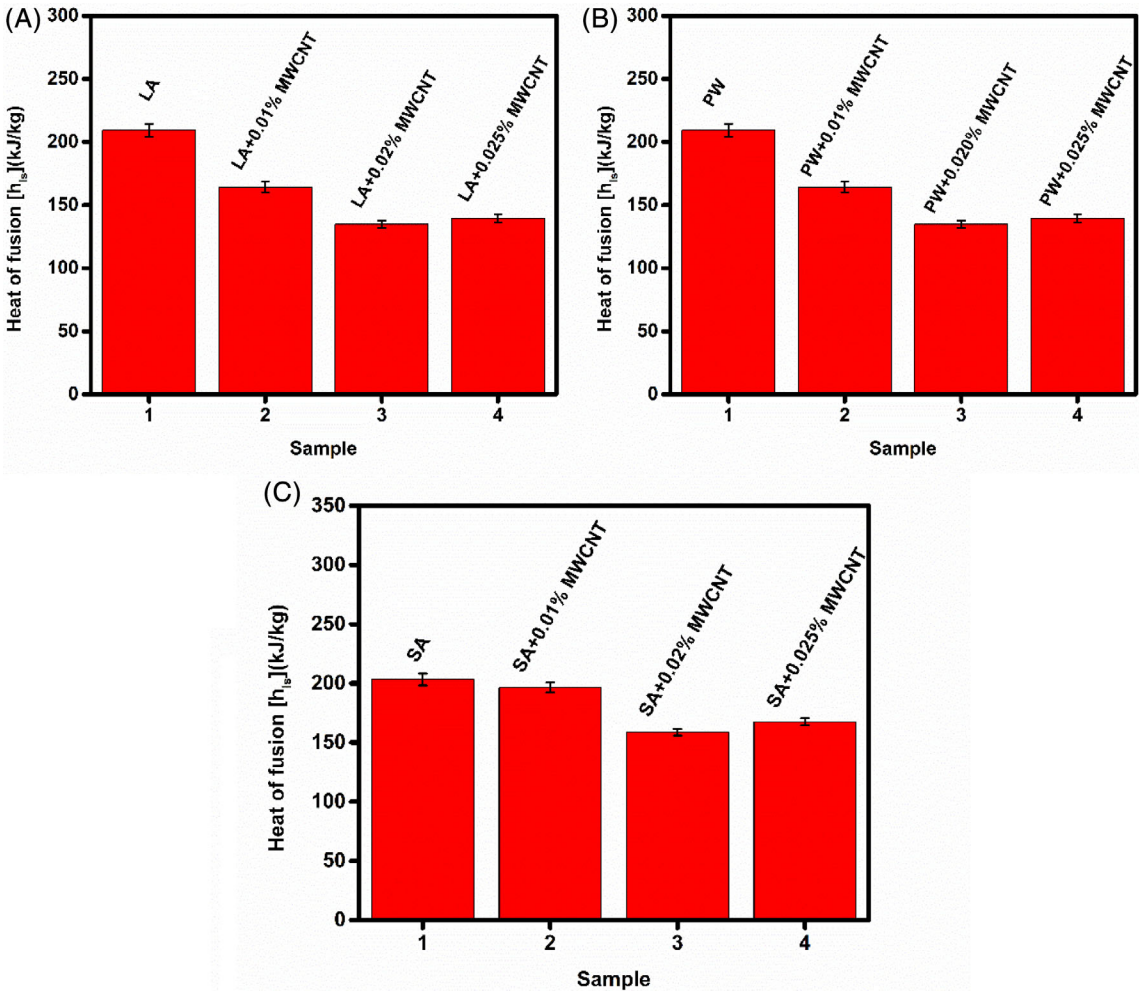

FIGURE 7 A, The latent heat of lauric acid PCM/NEPCM. B, The latent heat of paraffin wax PCM/NEPCM. C, The latent heat of stearic acid PCM/NEPCM

TABLE 5 Thermo-physical data obtained for 0.02% MWCNT based lauric acid, paraffin wax, and stearic acid NEPCMs by T-history method and hot disk analyzer

	The value obtained by the T-history method			The value obtained by Hot disk analyzer		
	LA + 0.02% MWCNT	PW + 0.02% MWCNT	SA + 0.02% MWCNT	LA + 0.02% MWCNT	PW + 0.02% MWCNT	SA + 0.02% MWCNT
C_{pl} [kJ/kg K]	3.02 ± 0.173	5.126 ± 0.206	3.452 ± 0.195	2.92 ± 0.154	4.962 ± 0.186	3.256 ± 0.163
C_{ps} [kJ/kg K]	2.32 ± 0.14	4.159 ± 0.188	4.18 ± 0.176	2.03 ± 0.118	4.03 ± 0.167	3.856 ± 0.143
K_l [W/m K]	0.2538 ± 0.013	0.4202 ± 0.018	0.199 ± 0.0137	0.2365 ± 0.009	0.3956 ± 0.012	0.1652 ± 0.0098
K_s [W/m K]	0.298 ± 0.0098	0.4765 ± 0.0147	0.2294 ± 0.0121	0.2736 ± 0.006	0.432 ± 0.011	0.1986 ± 0.0087

3 | RESULT AND DISCUSSION

3.1 | Charging profile of PCM/NEPCM

The melting profile of pure LA, PW, and SA with 0.01%, 0.02%, and 0.025% volume fractions of MWCNT have been presented in Figure 2A-C. Results revealed that 0.02% vol. fraction MWCNT-based LA, PW, and SA required 300, 300, and 420 seconds less time than pure LA, PW, and SA phase change materials, respectively. Also, the melting time of the volume fraction 0.02% MWCNT-based LA, PW, and SA composite phase change materials required less time than other taken volume fractions of MWCNT-based NEPCM. It is also observed on the variation in a liquid fraction, which has been shown in Figure 3A-C.

3.2 | Solidification profile of PCM/NEPCM

The solidification profile of pure LA, PW, and SA phase change materials with the additive MWCNT by vol. fractions of 0.01%, 0.02%, and 0.025% have been shown in Figure 4A-C. Results revealed that 0.02% vol. fraction MWCNT in LA, PW, and SA composite phase change materials required 420, 600, and 900 seconds less time than LA, PW, and SA phase change materials, respectively. The reason may be reduced charging and discharging times for the addition of MWCNT additives in LA, PW, and SA phase change materials. Also, it generally happens due to the reduction in the heat of fusion of PCMs/NEPCMs. However, Figure 4D represents the temperature profile during the cooling process of distilled water at ambient temperature.

3.3 | Variation in thermophysical properties of PCM/NEPCM

The T-History method obtained the thermophysical properties for pure LA, PW, and SA phase change materials with 0.01%, 0.02%, and 0.025% MWCNT. A tremendous enhancement in the thermo-physical properties of lauric acid, paraffin wax, and stearic acid by mixing MWCNT additives was observed. It has been established that a heat capacity (solid-state) of 0.02% MWCNT in LA, PW, and SA composite phase change materials was increased by 34.26%, 36.54%, and 25.86% than LA, PW, and SA phase change materials, respectively. The heat capacity (liquid state) of 0.02% MWCNT in LA, PW, and SA composite phase change materials increased by 15.71%, 62.57%, and 16% than LA, PW, and SA phase change materials, respectively, as shown in Figure 5A-C. Also, the heat capacity (liquid) of 0.02% MWCNT in paraffin

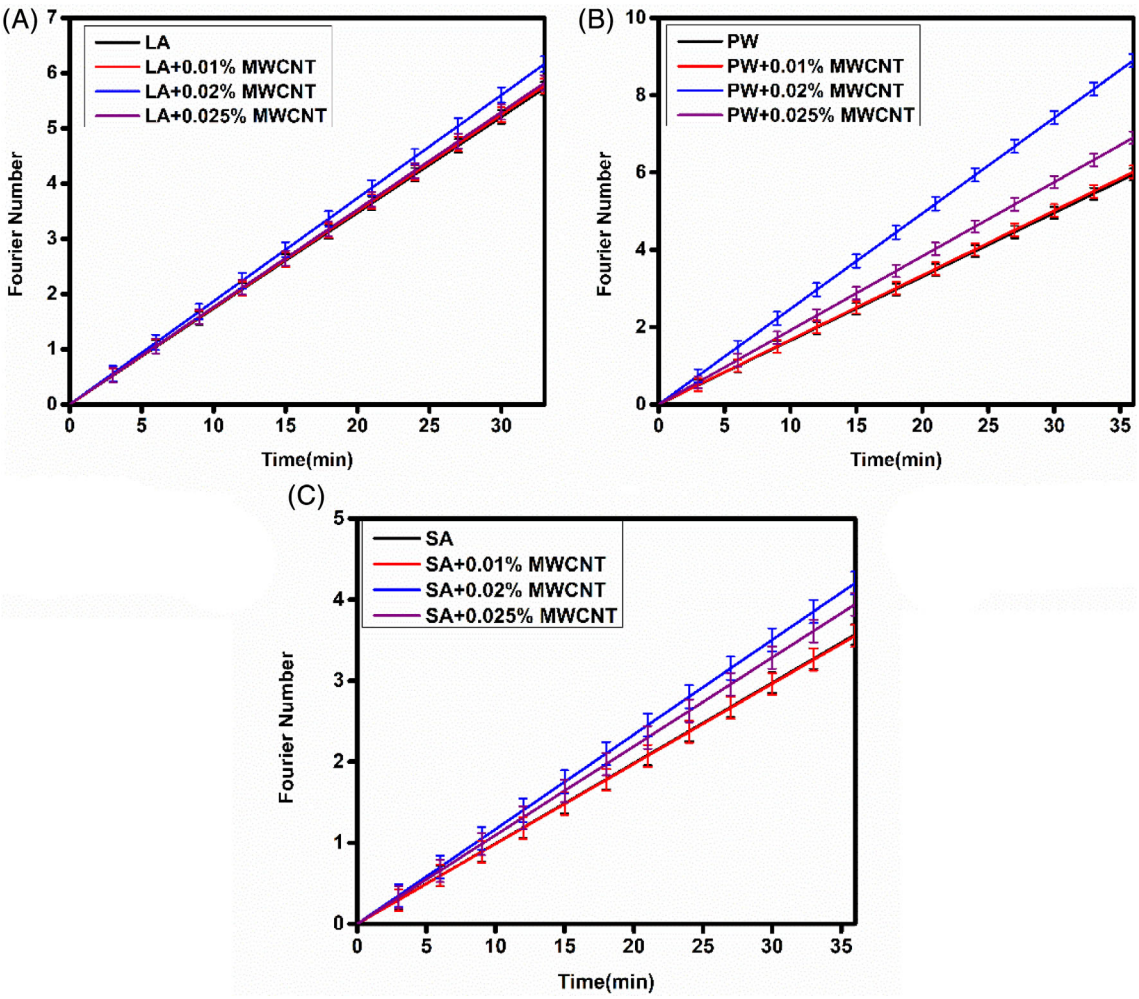

FIGURE 8 A, Fourier number of lauric acid PCM/NEPCM. B, Fourier number of paraffin wax PCM/NEPCM. C, Fourier number of stearic acid PCM/NEPCM.PCM/NEPCM

wax increased by 69.74% and 48.49% compared to 0.02% MWCNT in lauric acid stearic acid, respectively. The thermal conductivity (solid state) of 0.02% MWCNT in LA, PW, and SA composite phase change materials was increased by 37.8%, 24.4%, and 13.5% than LA, PW, and SA phase change materials, respectively. The thermal conductivity (liquid state) of 0.02% MWCNT in LA, PW, and SA composite phase change materials increased by 36.96%, 25.77%, and 13.45% than pure LA, PW, and SA phase change materials, respectively, as shown in Figure 6A-C. Also, the thermal conductivity (liquid and solid) of 0.02% MWCNT in paraffin wax was increased by 65.56%, 110.7%, 59.63%, and 107.71% than 0.02% MWCNT in lauric acid and stearic acid, respectively. Figure 7A-C showed the variation in the heat of fusion of pure LA, PW, and SA phase change materials with 0.01%, 0.02%, and 0.025% MWCNT. However, the present analysis revealed that the latent heat for 0.02% MWCNT LA, PW, and SA composite phase change materials were reduced by 8.55%, 35.95%, and 21.95% than pure LA, PW, and SA phase change materials, respectively. Also, the latent heat of 0.02% MWCNT in paraffin wax was reduced by 16.49% and 18.36% than 0.02% MWCNT in lauric acid and stearic acid, respectively. It was observed that within the volume fraction of MWCNT varied from 0% to 0.02% in LA, PW, and SA composite phase change materials; the thermo-physical properties have improved beyond the above vol. fraction the thermo-physical properties were decreased. This may happen due to the settlement of MWCNT particles after a volume fraction of 0.02% in LA, PW, and SA composite phase change materials. Also in the T-history approach and the hot disks analyzer were used to collect comparative thermo-physical properties data for 0.02% MWCNT-based LA, PW, and SA composite PCMs as shown in Table 5.

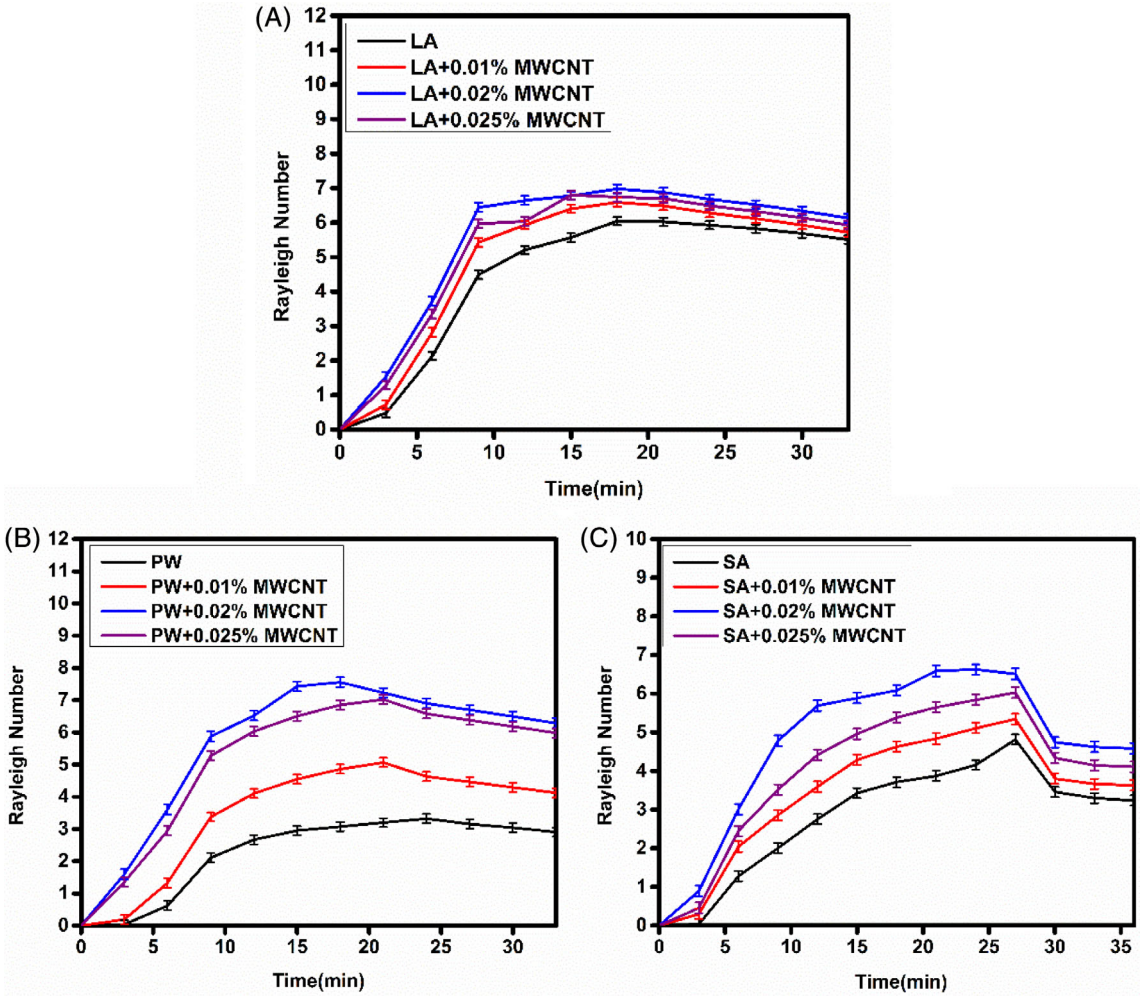

FIGURE 9 A, Rayleigh number of lauric acid PCM/NEPCM. B, Rayleigh number of paraffin wax PCM/NEPCM. C, Rayleigh number of stearic acid PCM/NEPCM

3.4 | Variation in dimensionless numbers of PCM/NEPCM

The variation in the Fourier number of pure and MWCNT-based LA, PW, and SA composite phase change materials has been presented in Figure 8A-C. The Fourier number is used to describe and forecast the temperature response of materials subjected to transient conductive heating or cooling. Results revealed that the maximum variation in Fourier number was obtained in the case of 0.02% MWCNT in LA, PW, and SA composite phase change materials. Figure 9A-C has shown the variation in Rayleigh number of LA, PW, and SA phase change materials with 0% to 0.025% MWCNT-based PCMs/NEPCMs. Rayleigh number is a dimensionless number associated with free or natural convection. From the experimental data, the variation of the Rayleigh number shows the heat transfer process is in natural convection. However, with an increase in the volume fraction of MWCNT from 0% to 0.02% in lauric acid, paraffin wax, and stearic acid PCMs, the variation in Rayleigh number increases and after then decreases. The maximum variation of Rayleigh number of 0.02% MWCNT-based LA, PW, and SA composite phase change materials was increased by 15.5%, 127.4%, and 27.34% than LA, PW, and SA phase change materials, respectively. Also, the maximum variation in Nusselt number for 0.02% MWCNT-based LA, PW, and SA composite phase change materials increased by 3.14%, 22.6%, and 8.33% than LA, PW, and SA phase change materials, respectively, as presented in Figure 10A-C. The ratio of convective to conductive heat transfer across the boundary is expressed as a Nusselt number, which is a dimensionless number. From the experiments, the Nusselt number varies from 0 to 31, which is justified by the heat transfer across the boundary by conduction and convection processes.

3.5 | Variation in heat transfer coefficient and heat transfer rate of PCM/NEPCM

Variation in heat transfer coefficient of MWCNT in PW and SA composite PCMs has been shown in Figure 11A-

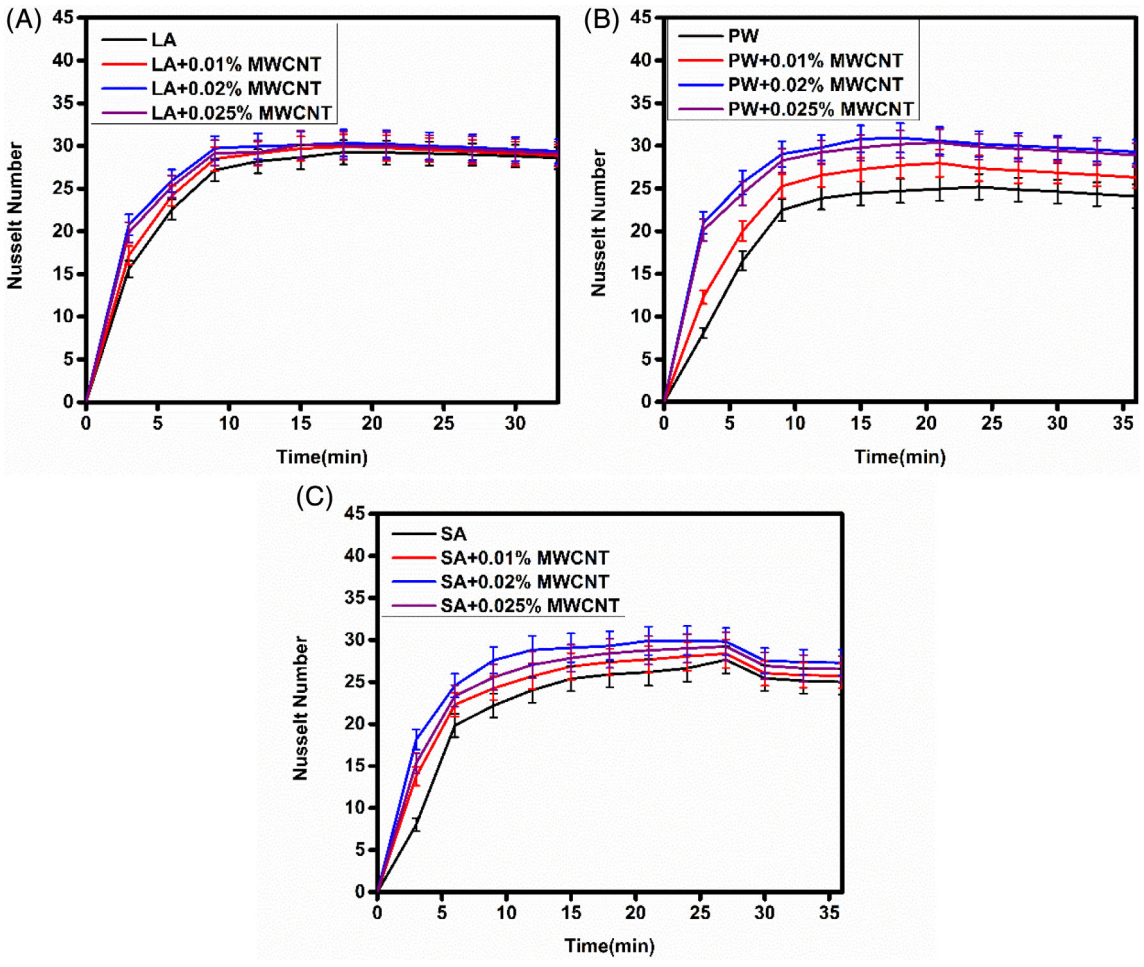

FIGURE 10 A, Nusselt Number of lauric acid PCM/NEPCM. B, Nusselt Number of paraffin wax PCM/NEPCM. C, Nusselt number of stearic acid PCM/NEPCM

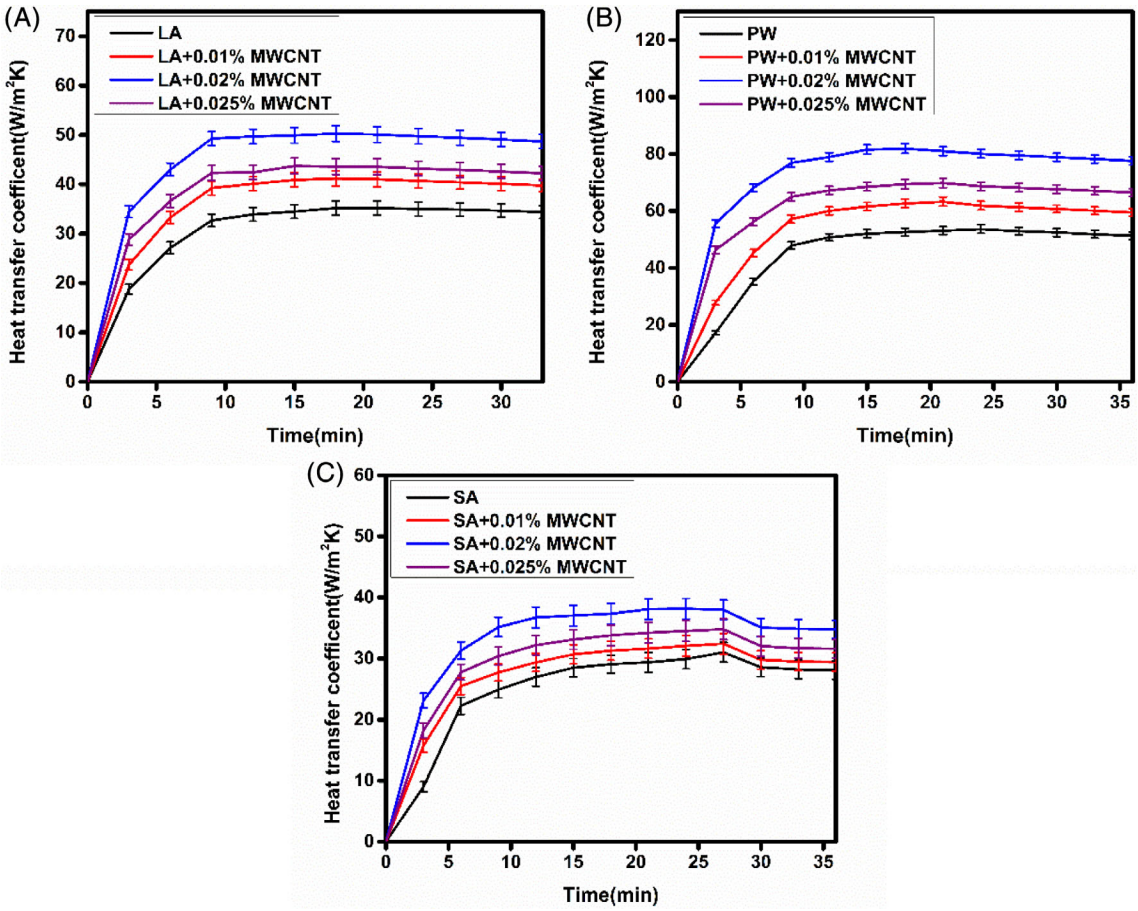

FIGURE 11 A, Heat transfer coefficient of lauric acid PCM/NEPCM. B, Heat transfer coefficient of paraffin wax PCM/NEPCM. C, Heat transfer coefficient of stearic acid PCM/NEPCM

C. Results revealed that 0.02% MWCNT in LA, PW, and SA composite PCMs obtained 42.89%, 52.8%, and 22.9% maximum changes in heat transfer coefficient than LA, PW, and SA PCMs. Also, the leading heat transfer coefficient of 0.02% MWCNT in paraffin wax increased by 62.8% and 114.9% than 0.02% MWCNT in LA and SA, respectively. It has been revealed that the heat transfer rate during the charging process of 0.02% MWCNT in LA, PW, and SA composite phase change materials increased by 61.16%, 87%, and 26.4% than LA, PW, and SA PCMs presented in Figure 12A-C. It may be happened due to the reduction in the latent heat and increment in thermal conductivity with the addition of MWCNT from 0% to 0.02% volume fraction-based LA, PW, and SA composite phase change materials. Also, the maximum heat transfer for 0.02% MWCNT in paraffin wax was increased by 37.2% and 215%, then 0.02% MWCNT in lauric acid and stearic acid, respectively based thermal energy storage.

From the above experimental study, it has been revealed that 0.02% volume fraction MWCNT nano-additives in LA, PW, and SA composite phase change materials has shown an optimum result than pure LA, PW, and SA PCMs. Also, 0.02% MWCNT in PW has better thermophysical parameters than 0.02% MWCNT in NEPCMs containing lauric acid or stearic acid phase change material-based thermal energy storage.

4 | CONCLUSIONS

The thermophysical properties and thermal performance of the TES system with 0% to 0.025% MWCNT-based LA, PW, and SA composite PCMs were investigated in this article. It may be concluded that after adding 0.02% MWCNT in the pure PCMs, some quantity of particles settled down at the bottom of the tube. Due to this, optimum results were obtained at 0.02% MWCNT-based PCMs/NEPCMs. The melting time of 0.02% MWCNT-based LA, PW, and SA composite PCMs reduced by 420, 600, and 900 seconds time than LA, PW, and SA phase change materials. The maximum solidification time also decreased by adding 0.02% MWCNT-based LA, PW, and SA composite PCMs Fourier number during the

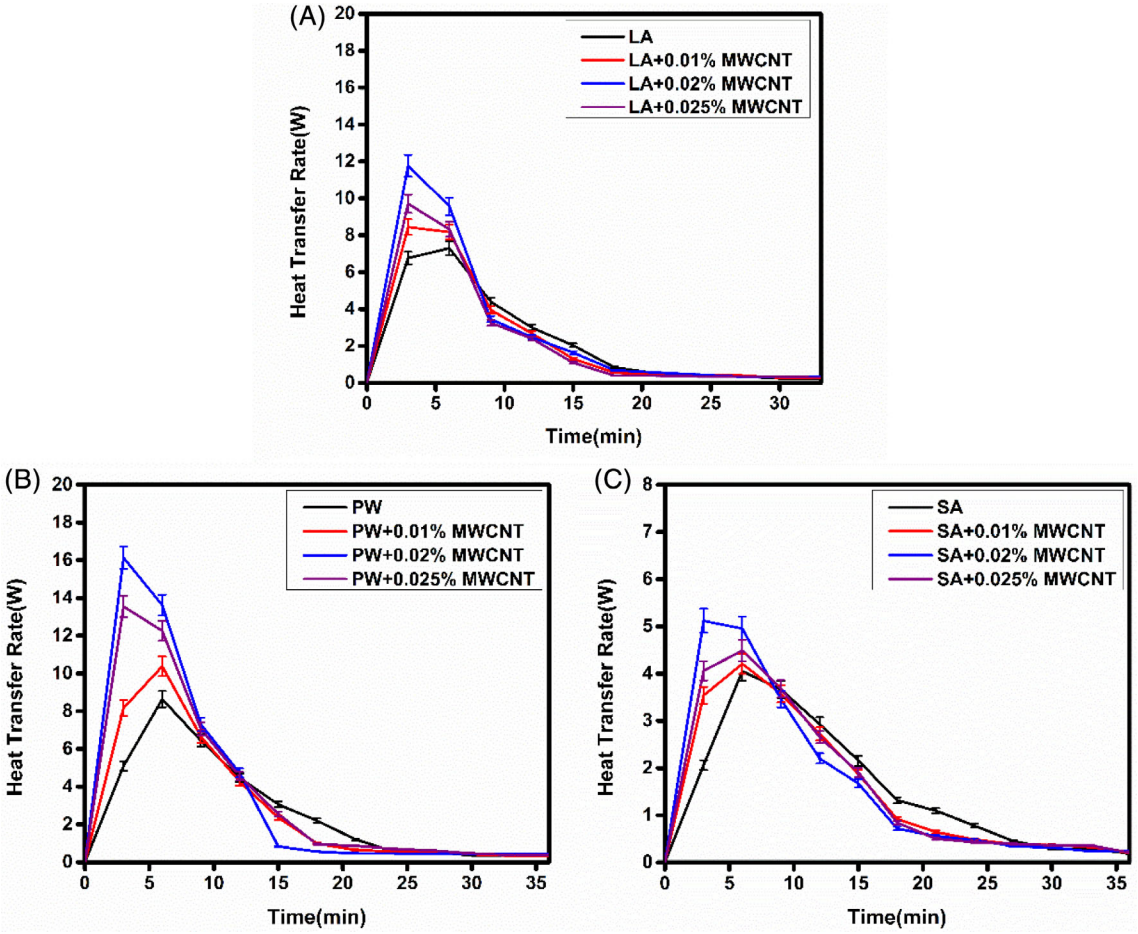

FIGURE 12 A, Heat transfer rate of lauric acid PCM/NEPCM. B, Heat transfer rate of paraffin wax acid PCM/NEPCM. C, Heat transfer rate of stearic acid PCM/NEPCM

charging of PCMs/NEPCMs is 0 to 10, which identified the combined effect of conduction and convection heat transfer processes. Also, the natural convection heat transfer process occurs in the range of $0 < Ra < 10^6$. Also, the maximum variation in Nusselt number for 0.02% MWCNT in LA, PW, and SA composite phase change materials increased by 3.14%, 22.6%, and 8.33% than LA, PW, and SA phase change materials, respectively. The maximum heat transfer coefficient for 0.02% MWCNT in LA, PW, and SA composite phase change materials obtained 42.89%, 52.8%, and 22.9% maximum variation, respectively, then LA, PW, and SA phase change materials. The maximum variation in heat transfer rate during charging of 0.02% MWCNT-based LA, PW, and SA composite phase change materials have 61.16%, 87%, and 26.4% higher values than LA, PW, and SA phase change materials-based thermal energy storage system.

It was observed that the optimum level of MWCNT volume fraction-based paraffin wax and fatty acid organic phase change material had shown drastic improvement in the thermal performance of the TES system. The results of this study can be utilized to design effective TES-based waste heat recovery systems for automobiles and industrial applications. MWCNT composite PCM, with its remarkable thermal and electrical properties, tends to make TES more competitive. In the future, the benefits of using MWCNT in inorganic PCM may be explored, which would further help in the selection for high heat PCMs.

NOMENCLATURE

A_1 area between PCMs/NEPCMs and the room temperature profile corresponds to the liquid state of PCMs/NEPCMs

A_2 area between PCMs/NEPCMs and room temperature profile corresponding to the phase change state of PCMs/NEPCMs

A_3 area between PCMs/NEPCMs and the room temperature profile corresponds to the solid state of PCMs/NEPCMs

B_1 area between distilled water and room temperature profile corresponds to the liquid state of PCMs/NEPCMs

B_2	area between distilled water and room temperature profile corresponds to the phase change in the state of PCMs/NEPCMs
A	area (m^2)
Cp	heat capacity
Fo	Fourier number
T	temperature (K)
Nu	Nusselt number
Q	heat transfer rate (W)
R	radius of tube (m)
Ra	Rayleigh number
W	weight (kg)
T_m	melting point of PCMs/NEPCMs (K)
h_{ls}	heat of fusion of PCM (kJ/kg)
H	heat transfer coefficient (W/m^2 K)
G	earth gravity (m/s^2)
K	thermal conductivity (W/m K)
L	length (m)
M	mass (kg)
t_f	solidification time

SUBSCRIPTS

L	liquid
M	melting
Nep	nano-enhanced phase change material
Np	nanoparticles
O	origin
P	PCM
R	end
S	solid
T	tube
W	water

GREEK LETTERS

A	thermal diffusivity (m^2/s)
B	thermal expansion coefficient
Φ	volume fraction of MWCNT
M	dynamic viscosity (Pa s)
P	density (kg/m^3)

ORCID

Rashmi Rekha Sahoo https://orcid.org/0000-0003-3133-6626

REFERENCES

1. Hatami M, Ganji DD, Gorji-Bandpy M. A review of different heat exchangers designs for increasing the diesel exhaust waste heat recovery. *Renew Sustain Energy Rev*. 2014;37:168-181.
2. Jaguemont J, Omar N, Bossche PVD, Mierlo J. Phase-change materials (PCM) for automotive applications: a review. *Appl Therm Eng*. 2018;132:308-320.
3. Thermal Energy Storage Market by Technology (Sensible, Latent, Thermochemical), Storage Material (Water, Molten Salts, PCM), Application (Power Generation, District Heating & Cooling, Process Heating & Cooling), End User and Region—Global Forecast to 2025. https://www.marketsandmarkets.com/Market-Reports/thermal-energy-storage-market-61500371.html. [accessed August 10, 2021].
4. Advanced Phase Change Material (PCM) Market: Global Forecast (2010–2015) https://www.marketsandmarkets.com/Market-Reports/pcm-market-250.html. [accessed August 10, 2021].
5. Pielichowska K, Pielichowski K. Phase change materials for thermal energy storage. *Prog Mater Sci*. 2014;65:67-123.
6. Underwood CP, Shepherd T, Bull SJ, Joyce S. Hybrid thermal storage using coil-encapsulated phase change materials. *Energy Build*. 2018;159:357-369.
7. Qi L, Pan H, Zhu X, et al. A portable solar-powered air-cooling system based on phase-change materials for a vehicle cabin. *Energy Convers Manag*. 2017;150:148-158.
8. Cunha JPD, Eames P. Thermal energy storage for low and medium temperature applications using phase change materials—a review. *Appl Energy*. 2016;177:227-238.
9. Karthik M, Faik A, Rodriguez PB, Aseguinolaza JR, Aguanno BD. Preparation of erythritol–graphite foam phase change composite with enhanced thermal conductivity for thermal energy storage applications. *Carbon*. 2015;94:266-276.
10. Kumar R, Vyas S, Dixit A. Fatty acids/1-dodecanol binary eutectic phase change materials for low temperature solar thermal applications: design, development and thermal analysis. *Sol Energy*. 2017;155:1373-1379.
11. Gabriela De Paola M, Lopresto CG, Arcuri N, Calabrò V. Crossed analysis by T-history and optical light scattering method for Glauber's salt-based phase change materials performance evaluation. *J Dispers Sci Technol*. 2020;41:1-9. doi:10.1080/01932691.2020.1845193
12. Gabriela De Paola M, Lopresto CG, Arcuri N, Calabrò V. T-history method: the importance of the cooling chamber to evaluate the thermal properties of Glauber's salt-based phase change materials. *Measur Sci Technol*. 2020;32(3):035601.
13. Gabriela De Paola M, Lopresto CG. Waste oils and their transesterification products as novel bio-based phase change materials. *J Phase Change Mater*. 2021;1(1):1-8. doi:10.6084/jpcm.v1i1.6.
14. Li Y, Chen Y, Huang X, Jiang S, Wang G. Anisotropy-functionalized cellulose-based phase change materials with reinforced solar-thermal energy conversion and storage capacity. *Chem Eng J*. 2021;145:129086.
15. Yazici MY, Saglam M, Aydin O, Avci M. Thermal energy storage performance of PCM/graphite matrix composite in a tube-in-shell geometry. *Therm Sci Eng Prog*. 2021;23:100915. doi:10.1016/j.tsep.2021.100915
16. Agyenim F, Eames P, Smyth M. A comparison of heat transfer enhancement in a medium-temperature thermal energy storage heat exchanger using fins. *Sol Energy*. 2009;83:1509-1520.
17. Gasia J, Diriken J, Bourke M, Bael JV, Cabeza L. Comparative study of the thermal performance of four different shell-and-

tube heat exchangers used as latent heat thermal energy storage systems. *Renew Energy*. 2017;114:934-944.
18. Veismoradi A, Ghalambaz M, Shirivand H, et al. Study of paraffin-based composite-phase change materials for a shell and tube energy storage system: a mesh adaptation approach. *Appl Therm Eng*. 2021;190:116793. doi:10.1016/j.applthermaleng.2021.116793
19. Zhou H, Wei L, Cai Q, et al. Annulus eccentric analysis of the melting and solidification behavior in a horizontal tube-in-shell storage unit. *Appl Therm Eng*. 2021;190:116752. doi:10.1016/j.applthermaleng.2021.116752
20. Demirkıran IG, Cetkin E. Emergence of rectangular shell shape in thermal energy storage applications: fitting melted phase changing material in a fixed space. *J Energy Storage*. 2021;37:102455.
21. Asgari M, Javidan M, Nozari M, Asgari A, Ganji DD. Simulation of solidification process of phase change materials in a heat exchanger using branch-shaped fins. *Case Stud Therm Eng*. 2021;25:100835.
22. Yadav C, Sahoo RR. Thermal analysis comparison of nano-additive PCM-based engine waste heat recovery thermal storage systems: an experimental study. *J Therm Anal Calorim*. 2021:1-18. doi:10.1007/s10973-021-10611-x.
23. Yadav C, Sahoo RR. Effect of nano-enhanced PCM on the thermal performance of a designed cylindrical thermal energy storage system. *Exp Heat Transfer*. 2020;34:356-375. doi:10.1080/08916152.2020.1751744
24. Sopian K, Al-Waeli AHA, Kazem HA. Nano-enhanced fluids and latent heat storage material for photovoltaic modules: a case study and parametric analysis. *Int J Energy Res*. 2021;45:1-24.
25. Lin X, Zhang X, Ji J, Zheng L. Research progress on preparation, characterization, and application of nanoparticle-based microencapsulated phase change materials. *Int J Energy Res*. 2021;45(7):1-27.
26. Yu Q, Zhang C, Lu Y, et al. Comprehensive performance of composite phase change materials based on eutectic chloride with SiO_2 nanoparticles and expanded graphite for the thermal energy storage system. *Renew Energy*. 2021;172:1120-1132. doi:10.1016/j.renene.2021.03.061.
27. Yu Y, Zhao C, Tao Y, Chen X, He Y. Superior thermal energy storage performance of NaCl-SWCNT composite phase change materials: a molecular dynamics approach. *Appl Energy*. 2021;290:116799. doi:10.1016/j.apenergy.2021.116799
28. Yadav C, Sahoo RR. Experimental analysis for optimum thermal performance and thermophysical parameters of MWCNT based capric acid PCM by using the T-history method. *Powder Technol*. 2020;364:392-403.
29. Yadav C, Sahoo RR. Thermal performance analysis of MWCNT-based capric acid PCM thermal energy storage system. *J Therm Anal Calorim*. 2021;146:1539-1550. doi:10.1007/s10973-020-10186-z.
30. Zou D, Ma X, Liu X, Zheng P, Hu Y. Thermal performance enhancement of composite phase change materials (PCM) using graphene and carbon nanotubes as additives for the potential application in lithium-ion power battery. *Int J Heat Mass Transfer*. 2018;120:33-41.
31. Li X, Sheng X, Guo Y, et al. Multifunctional HDPE/CNTs/PW composite phase change materials with excellent thermal and electrical conductivities. *J Mater Sci Technol*. 2021;86:171-179.
32. Yadav C, Sahoo RR. Exergy, and energy comparison oforganic phase change materials based thermal energy storagesystem integrated with engine exhaust. *J Energy Storage*. 2019;24:100773. doi:10.1016/j.est.2019.100773
33. Yadav C, Sahoo RR. Energetic and exergetic investigation onlauric and stearic acid phase change material-based thermalenergy storage system integrated with engine exhaust. *Heat Trans Asian Res*. 2019;48(3):1-16. doi:10.1002/htj.21422.
34. Yinping Z, Yi J, Yi J. A simple method, the T-history method, of determining the heat of fusion, specific heat and thermal conductivity of phase-change materials. *Measur Sci Technol*. 1999;10:201-205.
35. Holman JP, Gajda WJ. *Experimental Methods for Engineers*. New York, NY: McGraw-Hill; 2001.
36. Shaikh S, Lafdi K, Hallinan K. Carbon nano additives to enhancelatent energy storage of phase change materials. *J Appl Phys*. 2008;103:094302-094306. doi:10.1063/1.2903538
37. Cao X, Yuan Y, Xiang B, Haghighat F. Effect of natural convectionon melting performance of eccentric horizontal shell and tubelatent heat storage unit. *Sustain Cities Soc*. 2018;38:571-581. doi:10.1016/j.scs.2018.01.025
38. Totala N, Shimpi M, Shete N, Bhopate V. Natural convection characteristics in a vertical cylinder. *Int J Eng Sci*. 2013;3:27-31.
39. Senthilraja S, Vijayakumar K, Gangadevi R. A comparativestudy on thermal conductivity of Al_2O_3/water, CuO/-water, and Al_2O_3–CuO/water nanofluids. *Digest J Nanomater Biostruct*. 2015;10(4):1449-1458.
40. Ebadi S, Tasnim SH, Aliabadi AA, Mahmud S. Melting of nano-PCM inside a cylindrical thermal energy storage system: a numerical study with experimental verification. *Energy Convers Manag*. 2018;166:241-259. doi:10.1016/j.enconman.2018.04.016

How to cite this article: Yadav C, Sahoo RR. Thermophysical properties and thermal performance evaluation of multiwalled carbon nanotube-based organic phase change materials using T-History method. *Int J Energy Res*. 2022;46(3):3115-3131. doi:10.1002/er.7368